Exons as units of phenotypic impact for truncating mutations in autism

Andrew H. Chiang[1,2,3], Jonathan Chang[1,2,3], Jiayao Wang[1,2], and Dennis Vitkup[1,2]*

[1] Department of Biomedical Informatics, Columbia University, New York, New York, USA
[2] Department of Systems Biology, Center for Computational Biology and Bioinformatics, Columbia University, New York, New York, USA
[3] These authors contributed equally to this work
Correspondence to DV at dv2121@columbia.edu

Abstract

Autism spectrum disorders (ASD) are a group of related neurodevelopmental diseases displaying significant genetic and phenotypic heterogeneity[1-4]. Despite recent progress in understanding ASD genetics, the nature of phenotypic heterogeneity across probands remains unclear[5,6]. Notably, likely gene-disrupting (LGD) *de novo* mutations affecting the same gene often result in substantially different ASD phenotypes. Nevertheless, we find that truncating mutations that affect the same exon frequently lead to strikingly similar intellectual phenotypes in unrelated ASD probands. Analogous patterns are observed for two independent proband cohorts and several other important ASD-associated phenotypes. These results suggest that exons, rather than genes, often represent a unit of effective phenotypic impact for truncating mutations in autism. The observed phenotypic effects are likely mediated by nonsense-mediated decay (NMD) of splicing isoforms, with autism phenotypes usually triggered by relatively mild (15-30%) decreases in overall gene dosage. We find that exons with biases towards prenatal and postnatal expression preferentially contribute to ASD cases with lower and higher IQ phenotypes, respectively. We further demonstrate that LGD mutations in the same exon usually lead to similar expression changes across human tissues. Therefore, analogous phenotypic patterns may be also observed in other genetic disorders.

In this study, we focused on severely damaging, so-called likely gene-disrupting (LGD) mutations, which include nonsense, splice site, and frameshift variants. We used genetic and phenotypic data, including exome *de novo* mutations and corresponding phenotypes of ASD probands[7], for more than 2,500 families from the Simons Simplex Collection (SSC). *De novo* LGD mutations are observed at significantly higher rates in SSC probands compared to unaffected siblings[8,9]. This demonstrates a substantial contribution of these mutations to disease etiology in simplex ASD families[8], i.e. families with only a single affected child among siblings. We primarily considered in the paper the impact of *de novo* LGD mutations on several well-studied intellectual phenotypes: full-scale (FSIQ), nonverbal (NVIQ), and verbal (VIQ) intelligence quotients[8,10,11]. Notably, these scores are standardized by age and normalized across a broad range of phenotypes[7].

We first investigated the variability of intellectual phenotypes associated with *de novo* LGD mutations in the same gene. The IQ differences between probands with mutations in the same gene were slightly smaller than the differences between all pairs of probands. Specifically, the mean pairwise differences for probands with mutations in the same gene was 25.7 NVIQ points (~12% smaller compared to all pairs of ASD probands, Mann-Whitney U one-tail test $P = 0.14$; Supplementary Table 1). We next explored whether probands with LGD mutations at similar locations within the same gene resulted, on average, in more similar phenotypes (Supplementary Fig. 1). Indeed, IQ differences between probands with LGD mutations ≤ 1000 base pairs apart were significantly smaller than differences between probands with more distant mutations; ≤ 1 kbp NVIQ average difference 10.4 points; > 1 kbp average difference 28.6 points (MWU one-tail test $P = 0.005$). However, across the entire range of nucleotide distances between LGD mutations, we did not observe either a significant correlation or a monotonic relationship between IQ differences and mutation proximity (NVIQ Spearman's $\rho = 0.1$ $P = 0.4$; Mann-Kendall one-tail trend test $P = 0.5$).

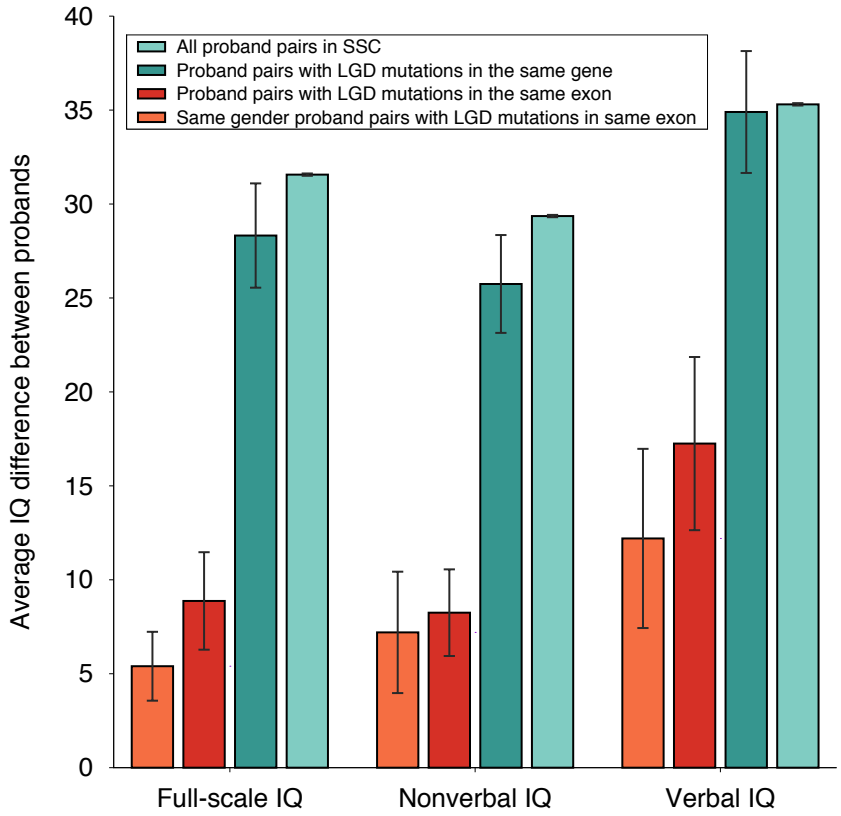

Figure 1: Average difference in IQ between SSC probands. Each bar shows the average IQ difference between pairs of probands from different groups. From right to left, the bars represent the average IQ difference between pairs of probands in the entire SSC population (light green), between probands with *de novo* LGD mutations in the same gene (dark green), between probands with *de novo* LGD mutations in the same exon (red), between probands of the same gender and with *de novo* LGD mutations in the same exon (orange). Error bars represent the SEM.

To explain the observed patterns of phenotypic similarity, we next considered the exon-intron structure of target genes. Specifically, we investigated truncating mutations affecting the same exon in unrelated ASD probands; we took into account LGD mutations in the exon's coding sequence as well as disruptions of the exon's flanking canonical splice sites, since such splice site mutations should affect the same transcript isoforms (Supplementary Fig. 2). Interestingly, the analysis of 16 unrelated ASD probands (8 pairs) with such mutations showed that they have strikingly more similar phenotypes (Fig. 1, red bars) compared to probands with LGD mutations in the same gene (Fig. 1, dark green bars); same exon FSIQ/NVIQ/VIQ average IQ difference 8.9, 8.3, 17.3 points, same gene average difference 28.3, 25.7, 34.9 points (Mann-Whitney U one-tail test P = 0.003, 0.005, 0.016). Because of well-known gender differences in autism susceptibility[11-13], we also compared IQ differences between probands of the same gender harboring truncating mutations in the same exon (Fig. 1, orange bars) to IQ differences between probands of different genders; same gender FSIQ/NVIQ/VIQ average difference 5.4, 7.2, 12.2; different gender average difference 14.7, 10, 25.7 (MWU one-tail test P = 0.04, 0.29, 0.07). Thus, stratification by gender further decreases the phenotypic differences between probands with LGD mutations in the same exon. Notably, the phenotypic similarity only extended to mutations in the same exon. The average IQ

differences between probands with LGD mutations in neighboring exons were not significantly different compared to mutations in non-neighboring exons (MWU one-tail test *P* = 0.6, 0.18, 0.8; Supplementary Fig. 3). The observed effects are also specific to LGD mutations; probands with either synonymous (P = 0.93, 0.97, 0.95; Supplementary Fig. 4) or missense (P = 0.8, 0.5, 0.8; Supplementary Fig. 5) mutations in the same exon were as phenotypically diverse as random pairs of ASD probands.

We next explored the relationship between phenotypic similarity and the proximity of truncating mutations in the corresponding protein primary sequences. This analysis revealed that probands with LGD mutations in the same exon often had similar IQs, despite being affected by truncating mutations separated by scores to hundreds of amino acids in protein sequence (Fig. 2a; Supplementary Fig. 6). Notably, probands with LGD mutations in the same exon were more phenotypically similar than probands with LGD mutations separated by comparable amino acid distances in the same protein (NVIQ distance-matched permutation test *P* = 0.002; Supplementary Fig. 7). We also investigated whether *de novo* mutations truncating a larger fraction of protein sequences resulted, on average, in more severe intellectual phenotypes. The analysis showed no significant correlations between the fraction of truncated protein and the severity of intellectual phenotypes (Fig. 2b); NVIQ Pearson's R =0.05 (*P* = 0.35; Supplementary Fig. 8). We also did not find any significant biases in the distribution of truncating *de novo* mutations across protein sequences compared with the distribution of synonymous *de novo* mutations (Kolmogorov-Smirnov two-tail test *P* = 0.9; Supplementary Fig. 9). It is possible that the lack of the correlation between phenotypic impact and the fraction of truncated gene is due to the signal averaging across different proteins. Therefore, for genes with recurrent mutations, we used a paired test to investigate whether truncating a larger fraction of the same protein leads to more severe phenotypes. This analysis also showed no significant differences (average NVIQ difference 0.24 points; Wilcoxon signed-ranked one-tail test *P* =0.44). Using the Pfam database[14] we also investigated whether mutations that truncate the same protein domain lead to more similar phenotypic differences. We found that mutations in different exons, even when truncating the same protein domain, resulted in phenotypes as different as due to random LGD mutations in the same gene (average NVIQ differences = 28.1; Supplementary Fig. 10).

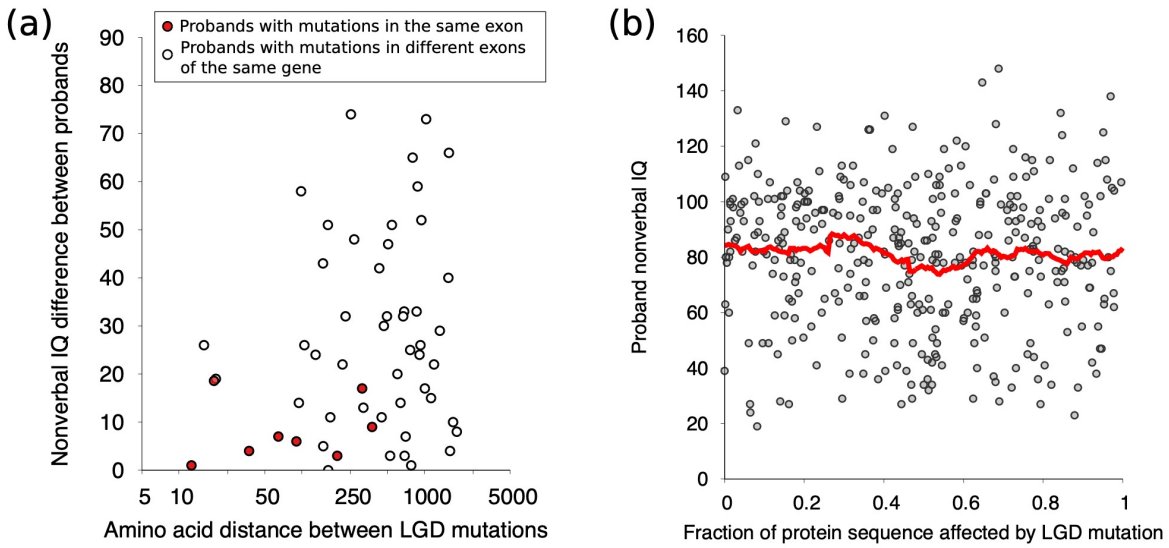

Figure 2: Amino acid position of *de novo* LGD mutations in protein sequence and probands' IQs. (**a**) Amino acid distance between LGD mutations in protein primary sequence versus differences in nonverbal IQ. Each point corresponds to a pair of probands with LGD mutations in the same gene. The x-axis represents the amino acid distance between LGD mutations, and the y-axis represents the difference between the corresponding probands' nonverbal IQs (NVIQ). Red points represent pairs of probands with LGD mutations in the same exon, and white points represent pairs of probands with mutation in the same gene but different exons. (**b**) Relative fraction of protein sequence truncated by LGD mutations versus probands' NVIQs. Each point corresponds to a single individual affected by an LGD mutation. The x-axis represents the fraction of protein sequence (i.e. fraction from the first amino acid) truncated by the mutation. The y-axis represents the corresponding NVIQ. Red line represents a moving average of the data.

The results presented above suggest that it is the occurrence of *de novo* LGD mutations in the same exon, rather than simply the proximity of mutation sites in nucleotide or amino acid sequence, that leads to similar phenotypic consequences. To explain this observation, we hypothesized that truncating mutations in the same exon usually affect, due to nonsense-mediated decay (NMD)[15], the expression of the same splicing isoforms. Therefore, such mutations should lead to similar functional impacts through similar effects on overall gene dosage and the expression levels of affected transcriptional isoforms. To explore this mechanistic model, we used data from the Genotype and Tissue Expression (GTEx) Consortium[16,17], which collected exome sequencing and human tissue-specific gene expression data from hundreds of individuals and across multiple tissues. Using ~4,400 LGD variants in coding regions and corresponding RNA-seq data, we compared the expression changes resulting from LGD variants in the same and different exons of the same gene (Fig. 3). For each truncating variant, we analyzed allele-specific read counts[18] and then used an empirical Bayes approach to infer the effects of NMD on gene expression (see Methods). This analysis demonstrated that the average gene dosage changes were more than 7 times more similar for individuals with LGD variants in the same exon compared to individuals with LGD variants in different exons of the same gene (Fig 3a); 2.2% versus 17.3% average difference in overall gene dosage decrease (Mann-Whitney U one-tail test $P < 2\times10^{-16}$). Moreover, by analyzing GTEx data for each tissue

separately, we consistently found drastically more similar dosage changes resulting from LGD variants in the same exons (Fig. 3a).

Distinct splicing isoforms often have different functional properties[19,20]. Consequently, LGD variants may affect phenotypes not only through NMD-induced changes in overall gene dosage, but also by altering the expression levels of different splicing isoforms. To analyze changes in the relative expression of specific isoforms, we used GTEx variants and calculated the angular distance metric between vectors describing isoform-specific expression changes (see Methods). This analysis confirmed that changes in relative isoform expression are significantly (~5 fold) more similar for LGD variants in the same exon compared to variants in different exons (Fig. 3b); 0.1 versus 0.46 average angular distance (Mann-Whitney U one-tail test $P < 2\times10^{-16}$). The results were also consistent across tissues (Fig. 3b). Overall, the analyses of GTEx data demonstrate that the changes in expression due to truncating variants in the same exon are indeed substantially more similar than the changes due to variants in different exons of the same gene.

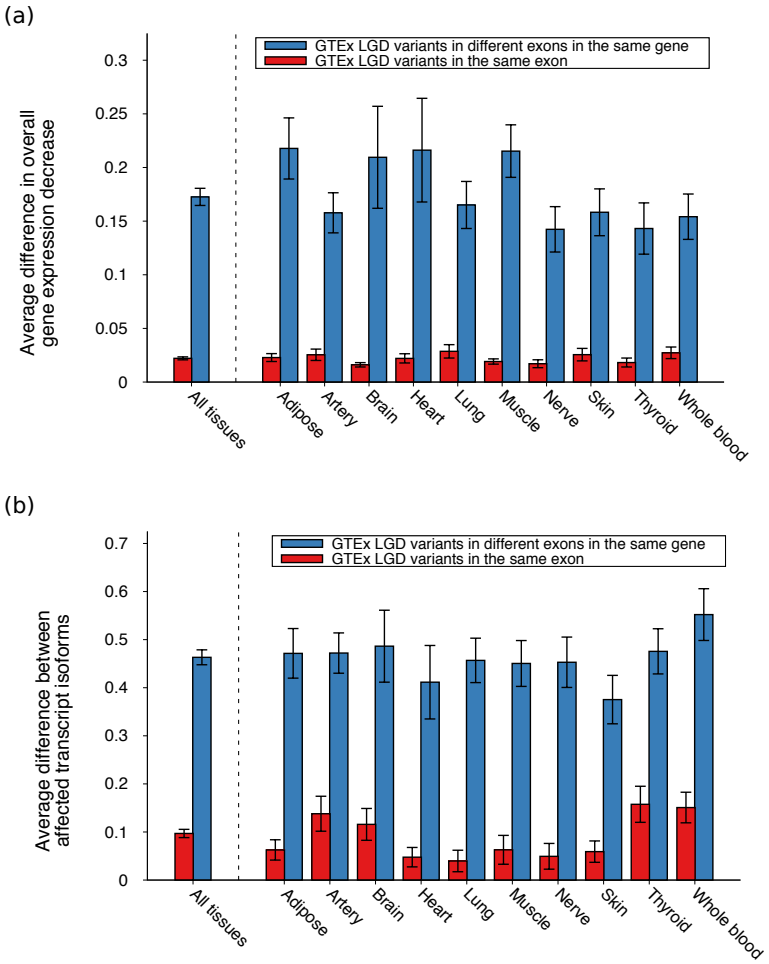

Figure 3: Gene expression changes due to LGD variants in the same exon and in the same gene but different exons. (**a**) Expression changes for genes harboring LGD variants were calculated based on data from the Genotype and Tissue Expression (GTEx) Consortium[16]. Bars represent the average difference in gene expression change between GTEx LGD variants in the same exon (red) and in the same gene but

different exons (blue) across human tissues. Error bars represent the SEM. (**b**) The average difference in isoform-specific expression change due to GTEx LGD variants. Differences in expression change across transcriptional isoforms were quantified using the angular distance metric between vectors representing isoform-specific expression changes. The average differences in isoform expression were calculated for LGD variants in the same exon (red bars) and in the same gene but different exons (blue bars) across human tissues. The height of each bar represents the average angular distance between isoform-specific expression changes across pairs of variants. Error bars represent the SEM.

Truncating variants in highly expressed exons should lead, through NMD, to relatively larger decreases in overall gene dosage. To confirm this hypothesis, we used RNA-seq data from GTEx to quantify the relative exon expression for each exon harboring a truncating variant. To calculate relative exon expression, we normalized GTEx expression values of each exon by GTEx expression values of the corresponding gene. Indeed, we observed a strong correlation between the relative expression levels of exons harboring LGD variants and the corresponding changes in overall gene dosage (Fig. 4; Pearson's R = 0.69, $P < 2\times10^{-16}$; Spearman's ρ = 0.81, $P < 2\times10^{-16}$; see Methods).

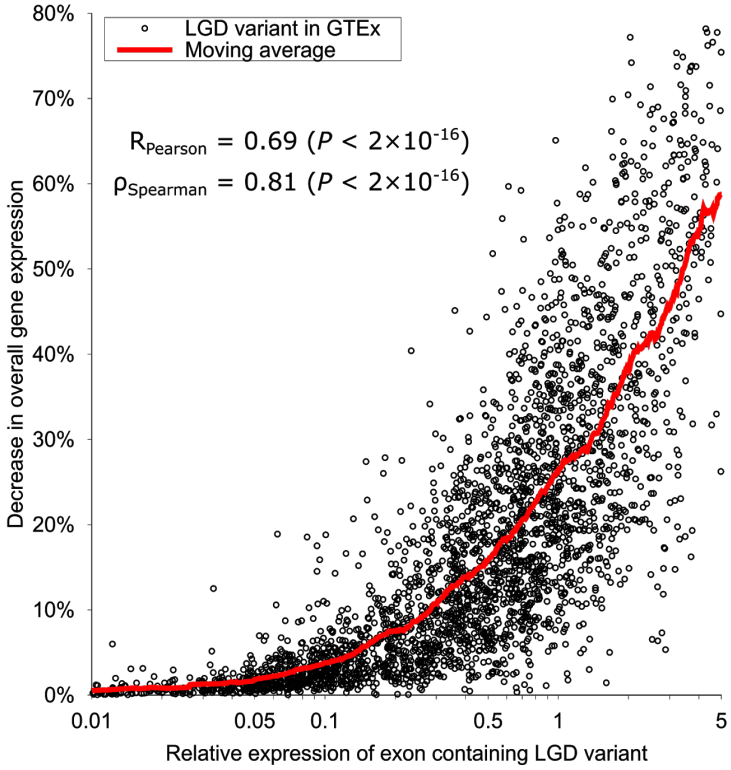

Figure 4: Relationship between the relative expression of exons containing LGD variants and the variant-induced decrease in overall gene expression. Each point corresponds to an LGD variant from the Genotype and Tissue Expression (GTEx) Consortium dataset, with gene and exon expression measured in one of ten human tissues. The x-axis represents the relative expression of the exon harboring the LGD variant in a tissue; the relative exon expression was calculated as the ratio between exon expression and total gene

expression (see Methods). The y-axis represents the decrease in overall gene expression due to nonsense-mediated decay (see Methods). Red line represents a moving average of the data.

Notably, NMD-induced dosage changes may mediate the relationship between the expression levels of target exons and the corresponding phenotypic effects of truncating mutations. To investigate this relationship we used the BrainSpan dataset[21], which contains exon-specific expression from human brain tissues. The BrainSpan data allowed us to estimate expression dosage changes resulting from LGD mutations in different exons of ASD-associated genes (see Methods). Notably, it is likely that there is substantial variability in the sensitivity of intellectual phenotypes to dosage changes across human genes. Therefore, to quantify the IQ sensitivities for genes with recurrent truncating mutations in SSC, we considered a simple linear dosage model. Specifically, we assumed that changes in probands' IQs are linearly proportional to decreases in gene dosage; we further assumed the average neurotypical IQ (100) for wild type gene dosage. We restricted our analysis to LGD mutations predicted to cause NMD-induced gene dosage changes, i.e. we excluded mutations within 50 bp of the last exon junction complex[22]. Using this model, we estimated the sensitivity of IQs to dosage changes for each gene with recurrent truncating ASD mutations (Supplementary Fig. 11; see Methods). Calculated in this way, the IQ sensitivity for a gene is equal to the estimated phenotypic effect of a truncating mutation in an exon with average expression.

The aforementioned model revealed that mutation-induced dosage changes are indeed strongly correlated with the normalized phenotypic effects; NVIQ Pearson's R = 0.63, permutation test P = 0.02; (Fig. 5a; Supplementary Fig. 12); very weak correlations were obtained using randomly permuted data, i.e. when truncating mutations were randomly re-assigned to different exons in the same gene (average NVIQ Pearson's R = 0.18; see Methods). Since the heritability of intelligence is known to significantly increase with age[23], we also investigated how the results depend on the age of probands. When we restricted our analysis to the older half of probands in SSC (median age 8.35 years), the strength of the correlations between the predicted dosage changes and normalized phenotypic consequences increased further; NVIQ Pearson's R = 0.75; permutation test P = 0.019 (Fig. 5b; Supplementary Fig. 13). The strong correlations between target exon expression and intellectual ASD phenotypes suggest that, when gene-specific effects are taken into account, a significant fraction (30%-40%) of the relative phenotypic effects of *de novo* LGD mutations can be explained by the resulting dosage changes in target genes.

Next, we evaluated the ability of our linear dosage model to explain the effects of LGD mutations on non-normalized IQs. For each gene with multiple truncating mutations, we used our regression model to perform leave-one-out predictions of each mutation's effect on proband IQ scores (Fig. 5c, inset; see Methods). Notably, for LGD mutations that trigger NMD, the inference errors of the dosage model were significantly smaller than the differences in IQ scores between probands with LGD mutations in the same gene; NVIQ median prediction error 11.0 points; same gene median IQ difference 22.0 points; MWU one-tail test P = 0.014 (Fig. 5c; Supplementary Fig. 14). The inference based on probands of the same gender had significantly smaller errors compared to inferences based on probands of the opposite gender, confirming functional differences in ASD genetics between genders; same gender NVIQ median error 9.1 points; different gender median error 19.9 points (MWU one-tail test P = 0.018). Moreover, the inference errors decreased for older probands; for example, for probands older than 12 years, median NVIQ error 7.6 points (Fig. 5c, Supplementary Fig. 14 and 15).

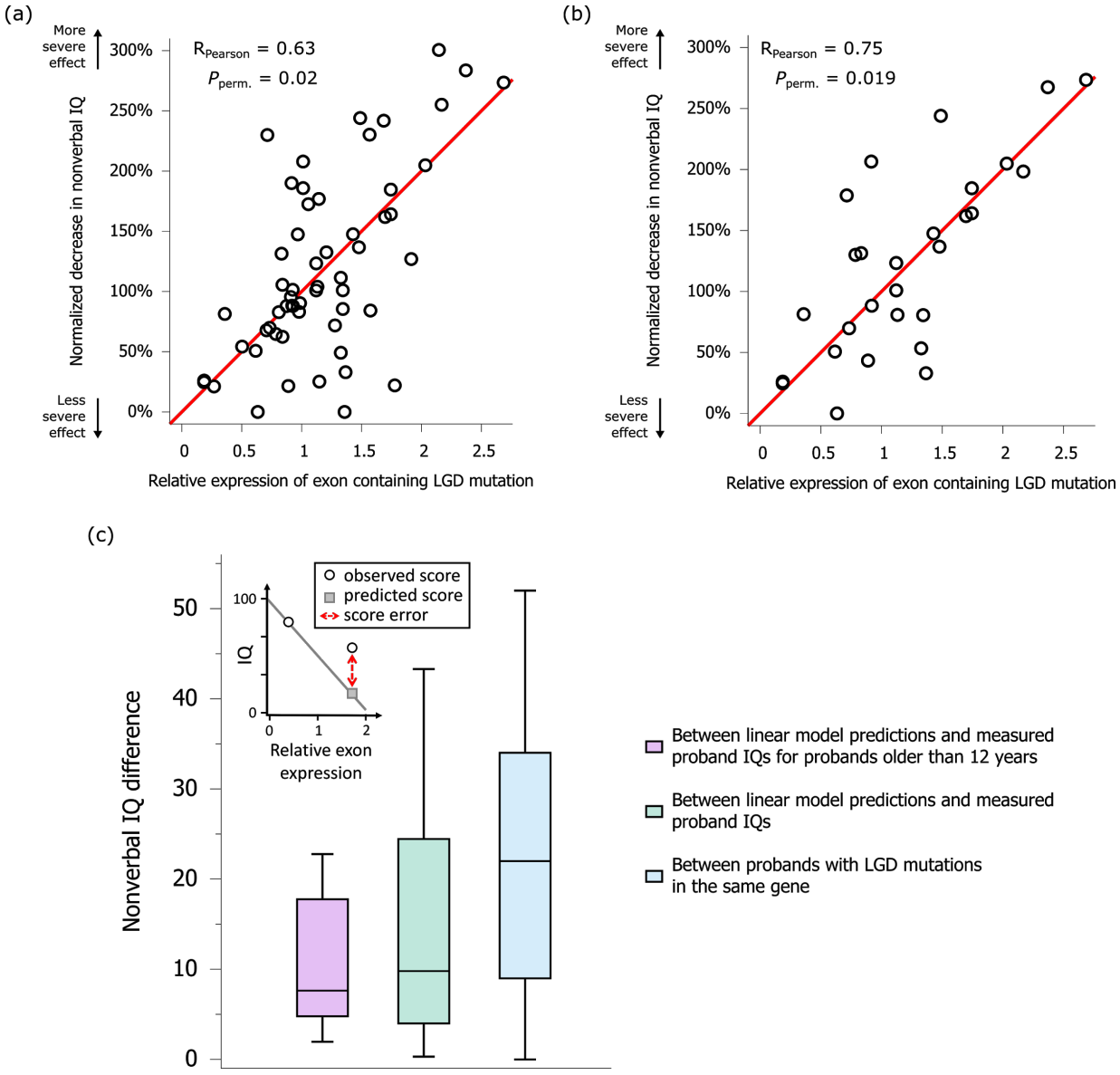

Figure 5: Relationship between the relative expression of exons harboring LGD mutations and the corresponding decrease in probands' intellectual phenotypes. (**a**) Each point corresponds to a proband with an LGD mutation in a gene; only genes with multiple LGD mutations in SSC were considered. The x-axis represents the relative expression (exon expression normalized by the total gene expression) of the exon harboring the LGD mutation. The y-axis represents the normalized effect of each mutation on the affected proband's nonverbal IQ (see Methods). The regression line across all points is shown in red. *P*-values were calculated based on randomly shuffled data (see Methods). (**b**) Same as (a), but with the analysis restricted to the older half of probands in SSC (median age 8.35 years). (**c**) Boxplots represent the distribution of errors in predicting the effects of LGD mutations on nonverbal IQ (see Methods) compared to the differences in IQ scores between probands with LGD mutations in the same gene (blue); prediction errors are shown for all probands (green) and for probands older than 12 years (purple). Only genes with multiple LGD mutations in SSC were considered. The ends of each solid box represent the upper and lower

quartiles; the horizontal lines inside each box represent the medians; and the whiskers represent the 5th and 95th percentiles. The inset panel illustrates the linear regression model used to perform leave-one-out predictions of proband IQs. Round open points represent measured scores for probands with LGD mutations in the same gene, the grey square point represents the predicted phenotypic score, and the red dotted line represents the prediction error.

Given that relative exon usage substantially changes across neural development[21,24], we next investigated the relationship between developmental profiles of exon expression and ASD phenotypes. To that end, we sorted exons from genes harboring LGD mutations[8] into four groups (quartiles) based on their developmental expression bias; the developmental bias was calculated as the fold change between prenatal and postnatal exon expression levels (Fig. 6a). We then analyzed the enrichment of LGD mutations in each exon group (see Methods). Notably, compared to exons with no substantial developmental bias, we found significant enrichment of LGD mutations not only in exons with a strong prenatal bias (binomial one-tail test $P = 8\times10^{-3}$, Relative Rate = 1.33), but also in exons with postnatal biases ($P = 0.018$, RR = 1.31) (Fig. 6b). To understand the origin of the observed biases, we stratified probands into lower (≤ 70) and higher IQ (> 70) cohorts (Fig. 6c). This analysis demonstrated that while LGD mutations associated with lower IQs were strongly enriched only in prenatally biased exons (binomial one-tail test $P = 6\times10^{-3}$, RR = 1.62), mutations associated with higher IQs displayed enrichment exclusively in postnatally biased exons ($P = 0.05$, RR = 1.27). These results reveal that mutations in exons with biases towards prenatal and postnatal expression preferentially contribute to ASD cases with lower and higher IQ phenotypes, respectively. Notably, the observed exon developmental biases for LGD mutations are not simply driven by biases at the gene level, as mutations associated with both higher and lower IQ phenotypes showed enrichment exclusively towards genes with prenatally biased expression (Supplementary Fig. 16).

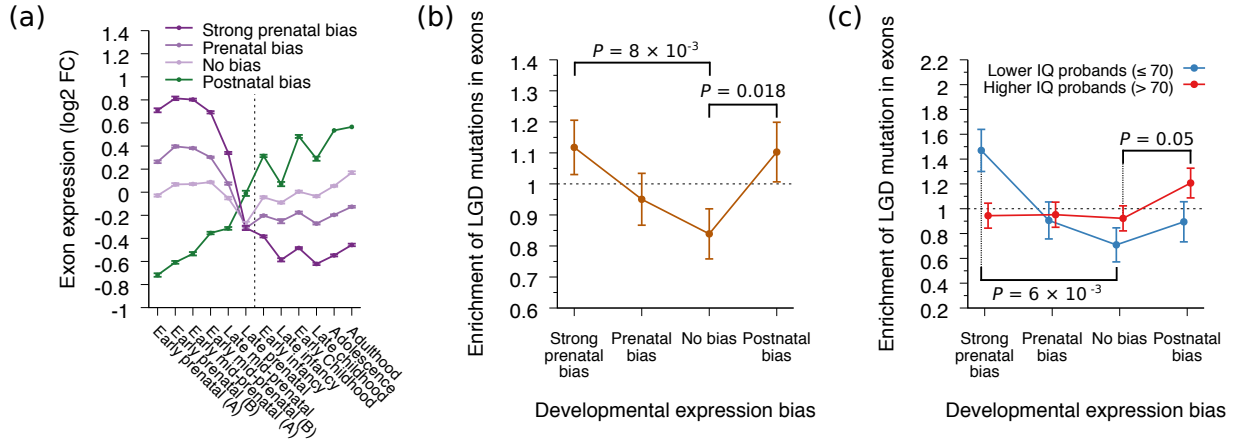

Figure 6: Relationship between the developmental expression of exons and intellectual ASD phenotypes. (**a**) Exon developmental expression profiles for genes with *de novo* LGD mutations in the Simons Simplex Collection (SSC). Exons from all genes harboring LGD mutations were sorted into four groups (strong prenatal bias, prenatal bias, no bias, and postnatal bias) based on their overall developmental expression bias; the developmental bias was calculated as the $\log_2$ fold change between average prenatal and

postnatal exon expressions. Lines represent the average expression profiles of exons in each group, and the x-axis represents 12 periods of human brain development, based on data from the Allen Institute's BrainSpan atlas [21]. Error bars represent the SEM. (**b**,**c**) Enrichment of LGD mutations across the four exon groups (x-axes) with different developmental biases. The y-axes represent the enrichment (relative rate) of mutations in each exon group; the mutation enrichment was calculated by randomizing LGD mutations across the corresponding gene lengths (see Methods). Error bars represent the SEM. (**b**) The overall enrichment of LGD mutations across groups of exons with different developmental expression biases. (**c**) The enrichment of LGD mutations across exon groups for ASD probands with higher IQ (>70, red) and lower IQ (<70, blue) phenotypes.

Although we primarily analyzed the impact of autism mutations on intellectual phenotypes, similar dosage and isoform expression changes in affected genes may also lead to analogous patterns for other quantitative ASD phenotypes[25,26]. Indeed, for LGD mutations predicted to lead to NMD, we observed similar results for several other key phenotypes. Specifically, probands with truncating mutations in the same exon exhibited more similar adaptive behavior abilities compared to probands with mutations in the same gene (Fig. 7a, Supplementary Fig. 17); Vineland Adaptive Behavior Scales (VABS)[27] composite standard score difference 4.7 versus 12.1 points (Mann-Whitney U one-tail test P = 0.017). In contrast, VABS differences between probands with truncating mutations in the same gene were not significantly smaller than for randomly paired probands (Fig. 7a, Supplementary Fig. 17); 12.1 versus 13.7 points (11% smaller; MWU one-tail test P = 0.23; Fig. 7a). Probands with truncating mutations in the same exon displayed more similar motor skills; the Purdue Pegboard Test, 1.2 versus 3.0 for the average difference in normalized tasks completed with both hands (MWU one-tail test P = 0.02; Supplementary Fig. 18; see Methods). Coordination scores in the Social Responsiveness Scale questionnaire were also more similar in probands with mutation the in the same exon; 0.6 versus 1.1 for the average difference in normalized response (MWU one-tail test P = 0.05; Supplementary Fig. 19).

Finally, we sought to validate the observed phenotypic patterns using an independent cohort of ASD probands. To that end, we analyzed an independently collected dataset from the ongoing Simons Variation in Individuals Project (VIP)[28]. The analyzed VIP dataset contained genetic information and VABS phenotypic scores for 41 individuals with *de novo* LGD mutations in 12 genes. Reassuringly, and consistent with our findings in SSC, probands from the VIP cohort with truncating *de novo* mutations in the same exon also exhibited strikingly more similar VABS phenotypic scores compared to probands with mutations in the same gene (Fig. 7a, Supplementary Fig. 20); VABS composite standard score difference 6.0 versus 12.4 (Mann-Whitney U one-tail test P = 0.014). Similar to the SSC cohort, LGD mutations in neighboring exons did not result in more similar behavior phenotypes; VABS composite standard score average difference 13.6 points (MWU one-tail test P = 0.6). The fraction of truncated proteins also did not show significant correlation with the VABS scores of affected probands (Pearson's R = -0.08, P = 0.7). Overall, these results confirm the phenotypic patterns observed in the SSC cohort, indicating the generality of the reported findings.

Using VABS scores from both SSC and VIP, we next investigated whether, analogous to the IQ phenotypes (Fig. 3a), the similarity of VABS scores are primarily due to the presence of mutations in the same exon, rather than proximity of truncating mutations within the corresponding protein sequence. Indeed, LGD mutations in the same exon often resulted in similar adaptive behavior abilities even when the corresponding mutations were separated by hundreds of amino acids (Fig. 7b; Supplementary Fig. 21).

By comparing mutations in the same exon to mutations separated by similar amino acid distances in the same protein, we confirmed that probands with mutations in the same exon were significantly more phenotypically similar (permutation test $P = 3\times10^{-4}$; Supplementary Fig. 22; see Methods).

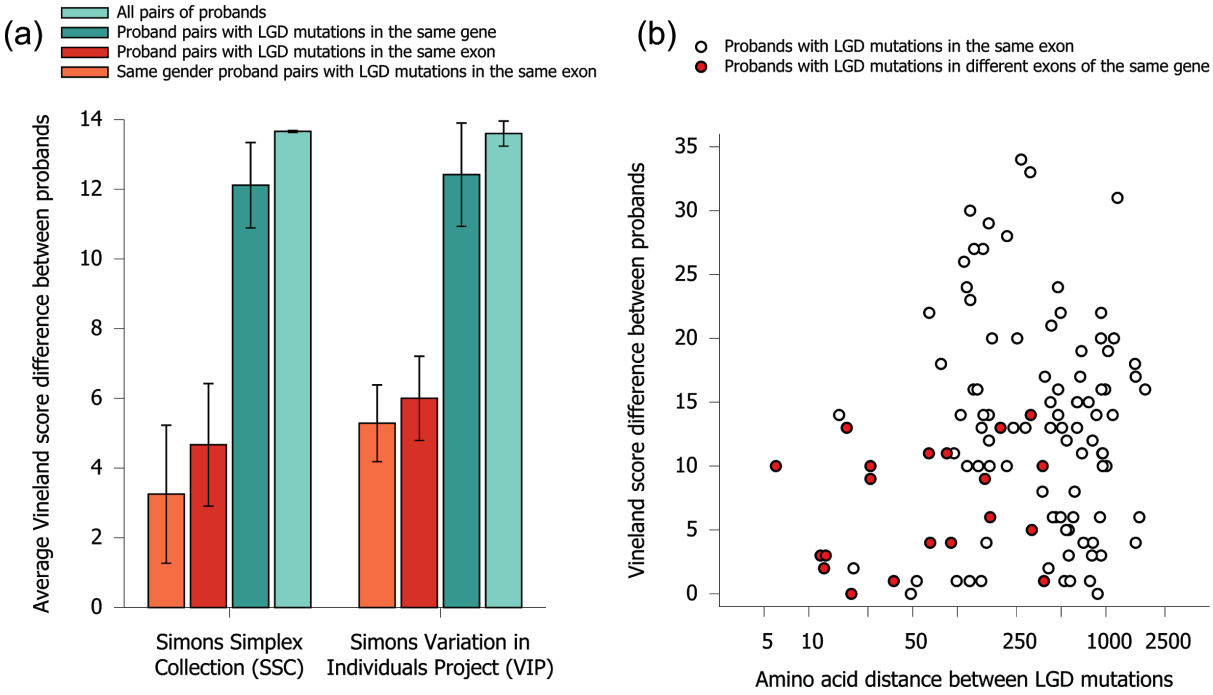

Figure 7: Vineland Adaptive Behavior Scales (VABS) score differences between probands using data from the Simons Simplex Collection (SSC) and the Simons Variation in Individuals Project (VIP). (**a**) Each bar shows the average difference in Vineland composite standard scores between pairs of probands in different groups. From right to left, bars represent differences between all pairs of probands in each cohort (light green), between probands with LGD mutations in the same gene (dark green), between probands with LGD mutations in the same exon (red), and between probands of the same gender with LGD mutations in the same exon (orange). Error bars represent the SEM. (**b**) Amino acid distance between LGD mutations versus differences in Vineland composite standard score. Each point corresponds to a pair of probands from either SSC or VIP with LGD mutations in the same gene. The x-axis represents the amino acid distance between LGD mutations, and the y-axis represents the difference between the affected probands' Vineland scores. Red points represent proband pairs with LGD mutations in the same exon, white points represent proband pairs with LGD mutations in different exons of the same gene. Only *de novo* LGD mutations that are predicted to trigger NMD are shown in the figures.

Discussion

Previous studies explored phenotypic similarity in syndromic forms of ASD due to mutations in specific genes[29-33]. Nevertheless, across a large collection of contributing genes, the nature of the substantial phenotypic heterogeneity in ASD remains unclear. Our study reveals several main sources of the observed heterogeneity in simplex ASD cases triggered by highly penetrant truncating mutations.

There is a substantial variability in the IQ sensitivity to dosage and isoform expression changes across human genes (Supplementary Fig. 11). We also estimate that, due to the imperfect efficiency of NMD, truncating mutations usually result in relatively mild changes in gene dosage, on average decreasing overall gene expression by ~15-30% (Supplementary Fig. 23; see Methods). Nevertheless, when gene-specific sensitivities are taken into account, the relative phenotypic effects are significantly correlated with expression dosage changes, which depend on the target exon expression (Fig. 5). Furthermore, even perturbations leading to similar dosage changes in the same gene may result in diverse phenotypes, if different functional isoforms are affected. We found that the similarity of truncated isoforms between LGD mutations significantly correlated with phenotypic similarity (NVIQ Spearman ρ= -0.21, P = 0.02; VABS Spearman ρ = -0.19, *P* = 0.006; see Methods). When exactly the same set of isoforms are perturbed, as is the case for LGD mutations in the same exon, the phenotypic diversity in unrelated probands decreases even further (Fig. 1). For intellectual phenotypes, same exon membership between LGD mutations accounts for a substantially larger fraction of phenotypic variance than multiple other genomic features, including expression, evolutionary conservation, pathway membership, and domain truncation (see Methods). Overall, these results demonstrate that for *de novo* LGD mutations, exons, rather than genes, represent a unit of effective phenotypic impact. It is also likely that differences in genetic background and environment represent other important sources of phenotypic variability[34-36]. As the heritability of IQ phenotypes usually increases with age, it is reassuring that we observe a substantially higher correlation between phenotypes and gene dosage changes for older probands (Fig. 5b).

In the present study, we focused specifically on simplex cases of ASD, in which *de novo* LGD mutations are highly penetrant. In more diverse cohorts, individuals with LGD mutations in the same exon will likely display substantially greater phenotypic heterogeneity. For example, the Simons Variation in Individuals Project identified broad spectra of phenotypes associated with specific variants in the general population[28,37-39]. We also observed significantly larger phenotypic variability for probands from sequenced family trios, i.e. families without unaffected siblings (Supplementary Fig. 24). For these probands, the enrichment of *de novo* LGD mutations is likely to be substantially lower and the contribution from genetic background larger[40], thus resulting in more pronounced phenotypic variability.

Our study may have important implications for precision medicine[34,41,42]. From a therapeutic perspective, compensatory expression of intact alleles, which has already been tested in mouse models of ASD[43-45] and other diseases[46], may provide an approach for alleviating phenotypic effects for at least a fraction of highly penetrant LGDs. From a prognostic perspective, our results suggest that by sequencing and phenotyping sufficiently large patient cohorts harboring truncating mutations in different exons of contributing ASD genes, it may be possible to understand likely phenotypic consequences, at least for a subset of cases resulting from highly penetrant *de novo* LGD mutations in simplex families. Furthermore, because we observe similar patterns of expression changes across multiple human tissues, medically relevant phenotypic analyses may be also extended to other disorders caused by highly penetrant truncating mutations.

References

1 American Psychiatric Association (DSM-5 Task Force). *Diagnostic and Statistical Manual of Mental Disorders: DSM-5*. 5th edn, (American Psychiatric Association, 2013).

2 Krumm, N., O'Roak, B. J., Shendure, J. & Eichler, E. E. A de novo convergence of autism genetics and molecular neuroscience. *Trends in Neurosciences* **37**, 95-105 (2014).

3 Ronemus, M., Iossifov, I., Levy, D. & Wigler, M. The role of de novo mutations in the genetics of autism spectrum disorders. *Nature Reviews Genetics* **15**, 133-141 (2014).

4 de la Torre-Ubieta, L., Won, H., Stein, J. L. & Geschwind, D. H. Advancing the understanding of autism disease mechanisms through genetics. *Nature Medicine* **22**, 345-361 (2016).

5 Jeste, S. S. & Geschwind, D. H. Disentangling the heterogeneity of autism spectrum disorder through genetic findings. *Nature Reviews Neurology* **10**, 74 (2014).

6 Talkowski, M. E., Minikel, E. V. & Gusella, J. F. Autism Spectrum Disorder Genetics: Diverse Genes with Diverse Clinical Outcomes. *Harvard Review of Psychiatry* **22** (2014).

7 Fischbach, G. D. & Lord, C. The Simons Simplex Collection: a resource for identification of autism genetic risk factors. *Neuron* **68**, 192-195 (2010).

8 Iossifov, I. *et al.* The contribution of de novo coding mutations to autism spectrum disorder. *Nature* **515**, 216-221 (2014).

9 Sanders, S. J. *et al.* De novo mutations revealed by whole-exome sequencing are strongly associated with autism. *Nature* **485**, 237-241 (2012).

10 O'Roak, B. J. *et al.* Sporadic autism exomes reveal a highly interconnected protein network of de novo mutations. *Nature* **485**, 246-250 (2012).

11 Chang, J., Gilman, S. R., Chiang, A. H., Sanders, S. J. & Vitkup, D. Genotype to phenotype relationships in autism spectrum disorders. *Nature Neuroscience* **18**, 191-198 (2015).

12 Fombonne, E. Epidemiology of Pervasive Developmental Disorders. *Pediatric Research* **65**, 591 (2009).

13 Robinson, E. B., Lichtenstein, P., Anckarsäter, H., Happé, F. & Ronald, A. Examining and interpreting the female protective effect against autistic behavior. *Proceedings of the National Academy of Sciences* **110**, 5258-5262 (2013).

14 El-Gebali, S. *et al.* The Pfam protein families database in 2019. *Nucleic Acids Research* **47**, D427-D432 (2018).

15 Chang, Y. F., Imam, J. S. & Wilkinson, M. F. The nonsense-mediated decay RNA surveillance pathway. *Annual Review of Biochemistry* **76**, 51-74 (2007).

16 GTEx Consortium. Human genomics. The Genotype-Tissue Expression (GTEx) pilot analysis: multitissue gene regulation in humans. *Science* **348**, 648-660 (2015).

17 Mele, M. *et al.* Human genomics. The human transcriptome across tissues and individuals. *Science* **348**, 660-665 (2015).

18 Rivas, M. A. *et al.* Human genomics. Effect of predicted protein-truncating genetic variants on the human transcriptome. *Science* **348**, 666-669 (2015).

19 Keren, H., Lev-Maor, G. & Ast, G. Alternative splicing and evolution: diversification, exon definition and function. *Nature Reviews Genetics* **11**, 345-355 (2010).

20 Yang, X. *et al.* Widespread expansion of protein interaction capabilities by alternative splicing. *Cell* **164**, 805-817 (2016).

21 Kang, H. J. *et al.* Spatio-temporal transcriptome of the human brain. *Nature* **478**, 483-489 (2011).

22 Nagy, E. & Maquat, L. E. A rule for termination-codon position within intron-containing genes: when nonsense affects RNA abundance. *Trends in Biochemical Sciences* **23**, 198-199 (1998).
23 Haworth, C. M. A. *et al.* The heritability of general cognitive ability increases linearly from childhood to young adulthood. *Molecular Psychiatry* **15**, 1112 (2009).
24 Weyn-Vanhentenryck, S. M. *et al.* Precise temporal regulation of alternative splicing during neural development. *Nature Communications* **9**, 2189 (2018).
25 Buja, A. *et al.* Damaging de novo mutations diminish motor skills in children on the autism spectrum. *Proceedings of the National Academy of Sciences* (2018).
26 Bishop, S. L. *et al.* Identification of Developmental and Behavioral Markers Associated with Genetic Abnormalities in Autism Spectrum Disorder. *The American Journal of Psychiatry* **174**, 576-585 (2017).
27 Zerbino, D. R. *et al.* Ensembl 2018. *Nucleic Acids Research* **46**, D754-D761 (2017).
28 Simons VIP Consortium. Simons Variation in Individuals Project (Simons VIP): a genetics-first approach to studying autism spectrum and related neurodevelopmental disorders. *Neuron* **73**, 1063-1067 (2012).
29 Sztainberg, Y. & Zoghbi, H. Y. Lessons learned from studying syndromic autism spectrum disorders. *Nature Neuroscience* **19**, 1408-1417 (2016).
30 Bernier, R. *et al.* Disruptive CHD8 mutations define a subtype of autism early in development. *Cell* **158**, 263-276 (2014).
31 Helsmoortel, C. *et al.* A SWI/SNF-related autism syndrome caused by de novo mutations in ADNP. *Nature Genetics* **46**, 380-384 (2014).
32 Van Bon, B. *et al.* Disruptive de novo mutations of DYRK1A lead to a syndromic form of autism and ID. *Molecular Psychiatry* (2015).
33 Ben-Shalom, R. *et al.* Opposing Effects on NaV1.2 Function Underlie Differences Between SCN2A Variants Observed in Individuals With Autism Spectrum Disorder or Infantile Seizures. *Biological Psychiatry* **82**, 224-232 (2017).
34 Gandal, M. J., Leppa, V., Won, H., Parikshak, N. N. & Geschwind, D. H. The road to precision psychiatry: translating genetics into disease mechanisms. *Nature Neuroscience* **19**, 1397 (2016).
35 Robinson, E. B. *et al.* Autism spectrum disorder severity reflects the average contribution of de novo and familial influences. *Proceedings of the National Academy of Sciences* **111**, 15161 (2014).
36 Robinson, E. B. *et al.* Genetic risk for autism spectrum disorders and neuropsychiatric variation in the general population. *Nature Genetics* **48**, 552 (2016).
37 Qureshi, A. Y. *et al.* Opposing brain differences in 16p11. 2 deletion and duplication carriers. *The Journal of Neuroscience* **34**, 11199-11211 (2014).
38 Hanson, E. *et al.* The cognitive and behavioral phenotype of the 16p11.2 deletion in a clinically ascertained population. *Biological Psychiatry* **77**, 785-793 (2015).
39 D'Angelo, D. *et al.* Defining the Effect of the 16p11.2 Duplication on Cognition, Behavior, and Medical Comorbidities. *JAMA Psychiatry* **73**, 20-30 (2016).
40 Zhao, X. *et al.* A unified genetic theory for sporadic and inherited autism. *Proceedings of the National Academy of Sciences* **104**, 12831 (2007).
41 Collins, F. S. & Varmus, H. A New Initiative on Precision Medicine. *New England Journal of Medicine* **372**, 793-795 (2015).
42 Geschwind, D. H. & State, M. W. Gene hunting in autism spectrum disorder: on the path to precision medicine. *The Lancet Neurology* **14**, 1109-1120 (2015).
43 Guy, J., Gan, J., Selfridge, J., Cobb, S. & Bird, A. Reversal of Neurological Defects in a Mouse Model of Rett Syndrome. *Science* **315**, 1143-1147 (2007).
44 Mei, Y. *et al.* Adult restoration of Shank3 expression rescues selective autistic-like phenotypes. *Nature* **530**, 481-484 (2016).

45 Ehninger, D. *et al.* Reversal of learning deficits in a Tsc2+/− mouse model of tuberous sclerosis. *Nature Medicine* **14**, 843 (2008).

46 Matharu, N. *et al.* CRISPR-mediated activation of a promoter or enhancer rescues obesity caused by haploinsufficiency. *Science* **363**, eaau0629 (2019).